# Jet and Photon Measurements using the ATLAS detector

Manuel Álvarez Estévez,
on behalf of the ATLAS Collaboration

Universidad Autónoma de Madrid
manuel.alvarez.estevez@cern.ch

PHENO 2020, May 4-6, 2020, Pittsburgh


# Introduction

The production of jets and prompt isolated photons provides stringent tests of perturbative, resummation and non-perturbative QCD and can be used to evaluate the proton PDFs.

---

**The production of jets** at high-$p_T$ is the dominant process in hadron colliders.

$\Rightarrow$ **Jet-substructure observables** characterize the radiation patterns in jets and display their internal properties for probing resummation or non-perturbative effects.

[arXiv:1912.09837] Soft-drop jet observables from 32.9 fb$^{-1}$ of data.
[arXiv:2004.03540] Lund jet plane from 139 fb$^{-1}$ of data.

---

**The production of photons** at high-$p_T$ proceeds via

- Hard interactions like $qg \rightarrow \gamma q$ and $q\bar{q} \rightarrow \gamma g$. $\Rightarrow$ Direct production.
- Fragmentation of hard partons like $q$ and $g$ into $\gamma$. $\Rightarrow$ Fragmentation production.
- Hadron decays, especially $\pi^0 \rightarrow \gamma\gamma$ decays.

$\Rightarrow$ **Prompt photons** are photons not coming from hadron decays.

[arXiv:1908.02746] Inclusive isolated-photon production from 36.1 fb$^{-1}$ of data.
[arXiv:1912.09866] Isolated-photon plus two-jet production from 36.1 fb$^{-1}$ of data.

---

All data sets from $pp$ collisions at $\sqrt{s} = 13$ TeV.

# Jet substructure techniques

**Grooming algorithms** remove constituents at wide angle and relatively soft.

⇒ **Soft-drop** for anti-$k_t$ jets with $R^{\text{jet}}$. Ref. [arXiv:1402.2657].

- Recluster the jet using Cambridge/Aachen and traverse clustering tree backwards.
- A pair of branches merges in each point where $j_1$ is the harder and $j_2$ the softer one.
- If a branch point satisfies the soft-drop condition from equation below, stop.
- Otherwise, remove the softer branch and continue down the harder one.

$$z_{j_1,j_2} = \frac{p_{\text{T},j_2}}{p_{\text{T},j_1} + p_{\text{T},j_2}} > z_{\text{cut}} \left( \frac{\Delta R_{j_1,j_2}}{R^{\text{jet}}} \right)^{\beta} \quad \text{where} \quad \Delta R_{i,j} = \sqrt{(\Delta y_{i,j})^2 + (\Delta \phi_{i,j})^2}$$

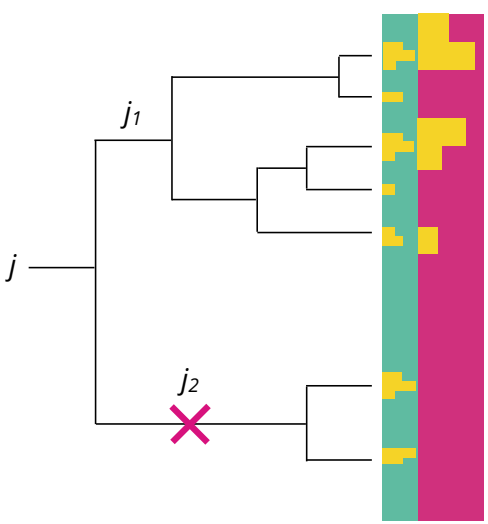


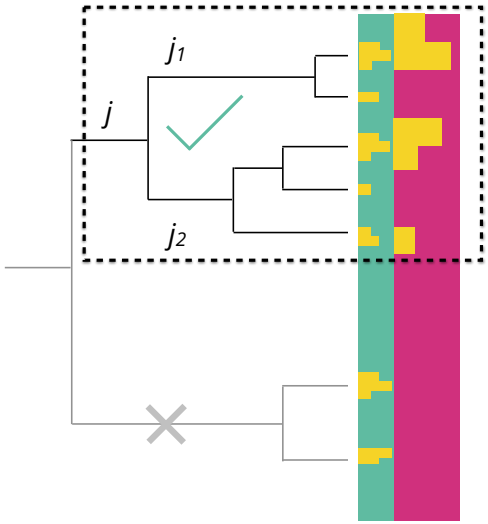

# Soft-drop jet observables

- $\rho \equiv \log_{10}(m^2_{\text{jet}}/p^2_{\text{T,jet}})$ where $m_{\text{jet}}$ is groomed and $p_{\text{T,jet}}$ is ungroomed.
- $z_g = p_{\text{T},j_2}/(p_{\text{T},j_1} + p_{\text{T},j_2})$
- $\log_{10}(r_g) = \log_{10}(\Delta R_{j_1,j_2})$

} for the splitting that satisfies the soft-drop condition.

---

- Anti-$k_t$ jets with $R^{\text{jet}} = 0.8$.
- Well-balanced dijet system: $p_{\text{T}}^{\text{jet}_1} > 300$ GeV and $p_{\text{T}}^{\text{jet}_1} < 1.5\, p_{\text{T}}^{\text{jet}_2}$ within $|\eta| < 1.5$.
- Calorimeter-based (all particles) and track-based (charged particles) definitions.
- Soft-drop grooming with $z_{\text{cut}} = 0.1$ and $\beta = 0$, 1 and 2.
- Iterative Bayesian unfolding technique.

PYTHIA 8.186: ME@LO with NNPDF2.3 LO, $p_{\text{T}}$-ordered PS, Lund string hadr. and A14 tune.

The MC predictions are mostly accurate except for the non-pertubative region.

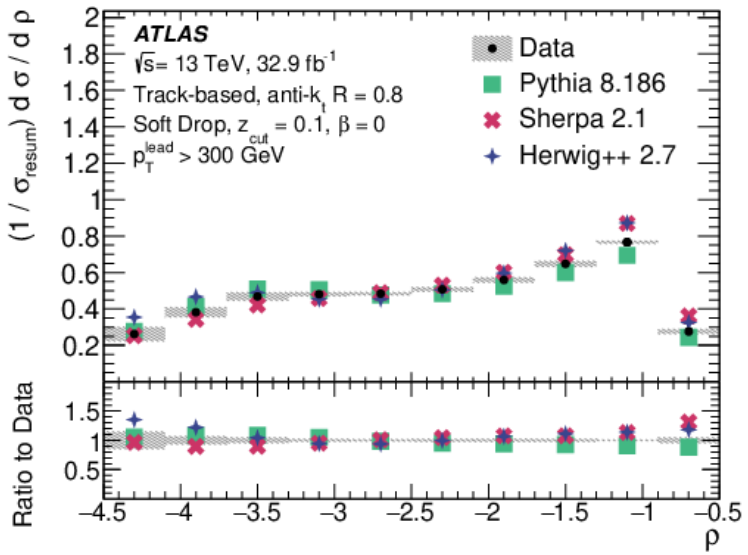


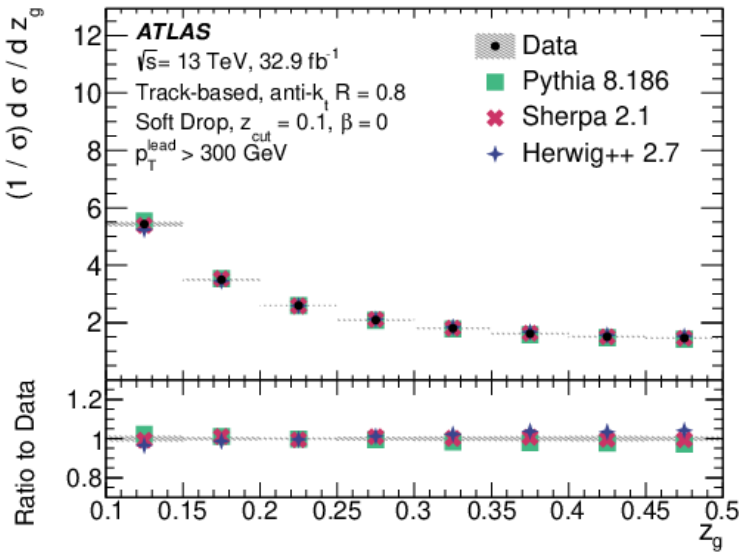


ATLAS Coll., arXiv:1912.09837

# Soft-drop jet observables

The calorimeter-based results are compared with all-particle analytical calculations:

- NNLL within SCET for $\rho$ including NP corrections. Ref. [arXiv:1803.03645].
- NLL within SCET for $\log_{10}(r_g)$. Ref. [arXiv:1908.01783].

This provides the first comparison between an analytical prediction and a measurement of $r_g$.

The calculations are able to model the data in the resummation region ($-3 < \rho < -1$) and the inclusion of NP effects improve the description in the non-perturbative region.

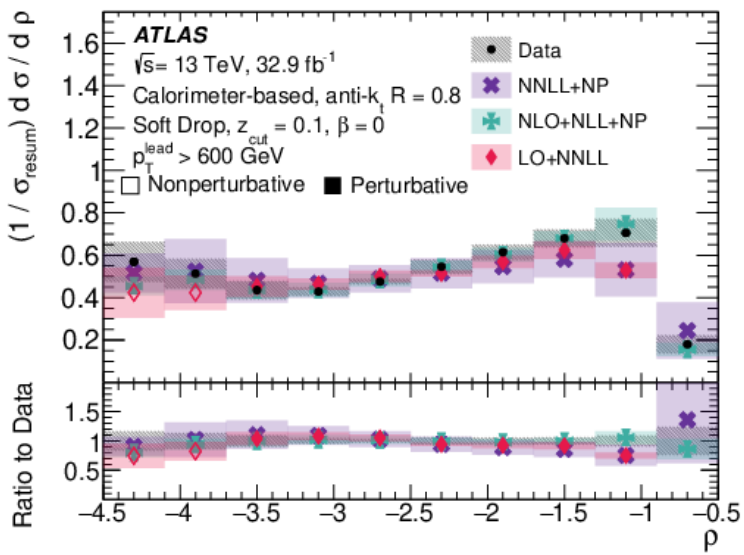


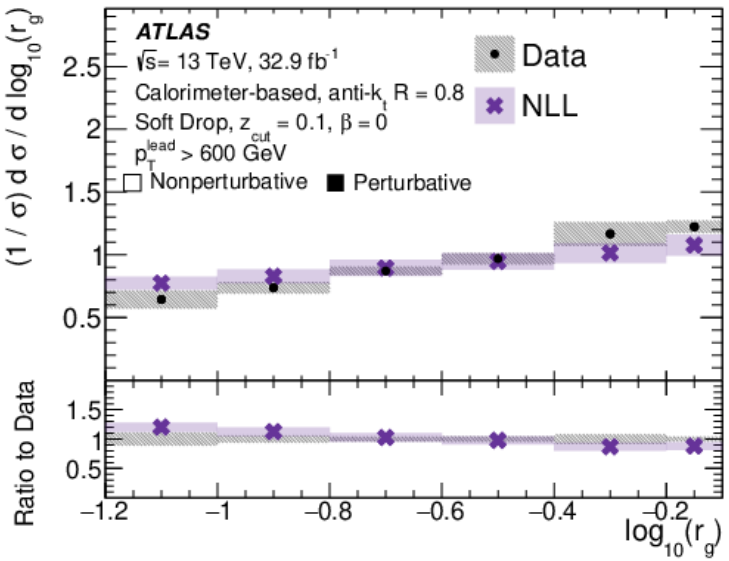


ATLAS Coll., arXiv:1912.09837

# Lund jet plane

The Lund plane encodes the emission pattern, $z$ being the momentum fraction of the emitted parton and $\theta$ the opening angle of the emission.

**Lund jet plane:** traverse Cambridge/Aachen clustering tree backwards following the harder branch and treat each branch point as a proxy for an emission.

$$z = \frac{p_{\mathrm{T,emission}}}{p_{\mathrm{T,core}} + p_{\mathrm{T,emission}}} \text{ and } \Delta R = \Delta R_{\mathrm{emission,core}} \Rightarrow \frac{1}{N_{\mathrm{jets}}} \frac{\mathrm{d}^2 N_{\mathrm{emissions}}}{\mathrm{d}\ln(1/z)\mathrm{d}\ln(R^{\mathrm{jet}}/\Delta R)}$$

The emission patterns from different physical processes are separated in the Lund jet plane.

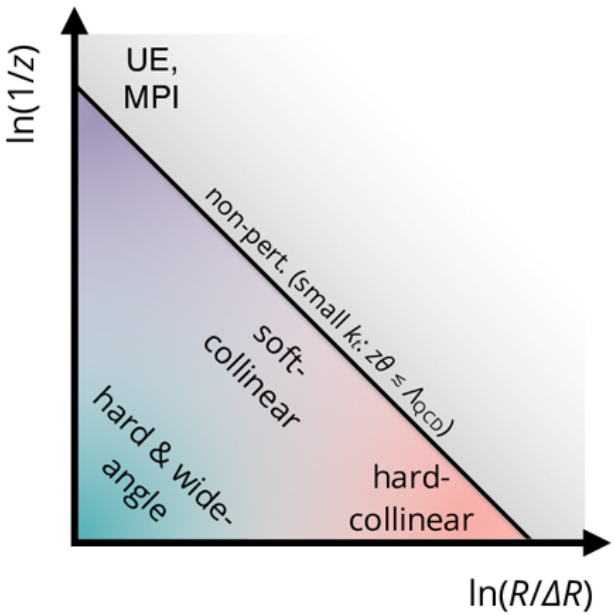


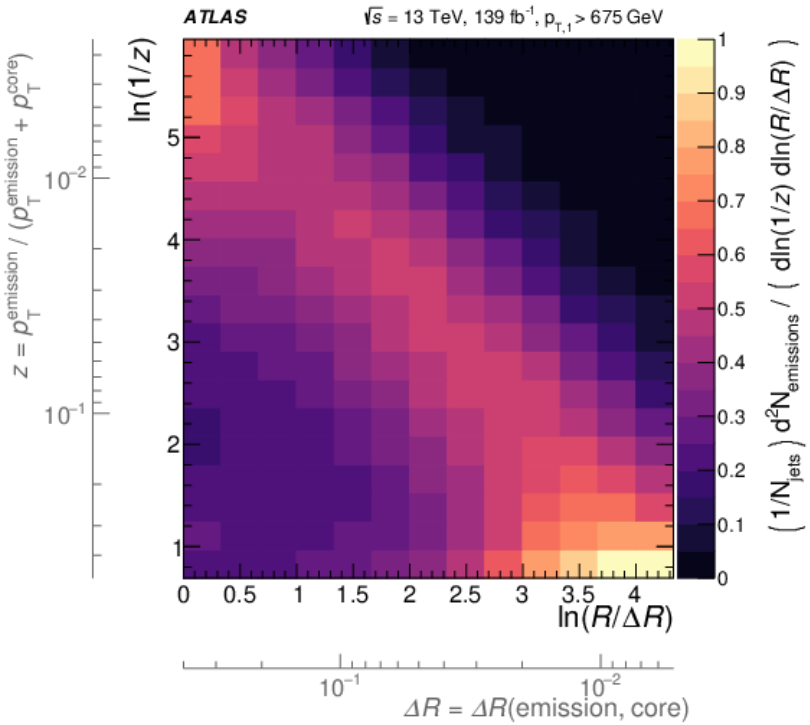


ATLAS Coll., arXiv:2004.03540

# Lund jet plane

⇒ Simultaneously useful for tuning non-perturbative models and for constraining advanced parton shower MC programs.

- Anti-$k_t$ jets with $R^{\text{jet}} = 0.4$.
- Well-balanced dijet system: $p_{\text{T}}^{\text{jet}_1} > 675$ GeV and $p_{\text{T}}^{\text{jet}_1} < 1.5\, p_{\text{T}}^{\text{jet}_2}$ within $|\eta| < 2.1$.
- Charged-particle tracks with $p_{\text{T}} > 500$ MeV and $\Delta R^{\text{track-jet}} < 0.4$ .
- Iterative Bayesian unfolding technique.

PYTHIA 8.186: ME@LO with NNPDF2.3 LO, $p_{\text{T}}$-ordered PS, Lund string hadr. and A14 tune.

No prediction describes the data accurately in all regions, but HERWIG 7.1.3 (Ang. ord.) provides overall the best description.

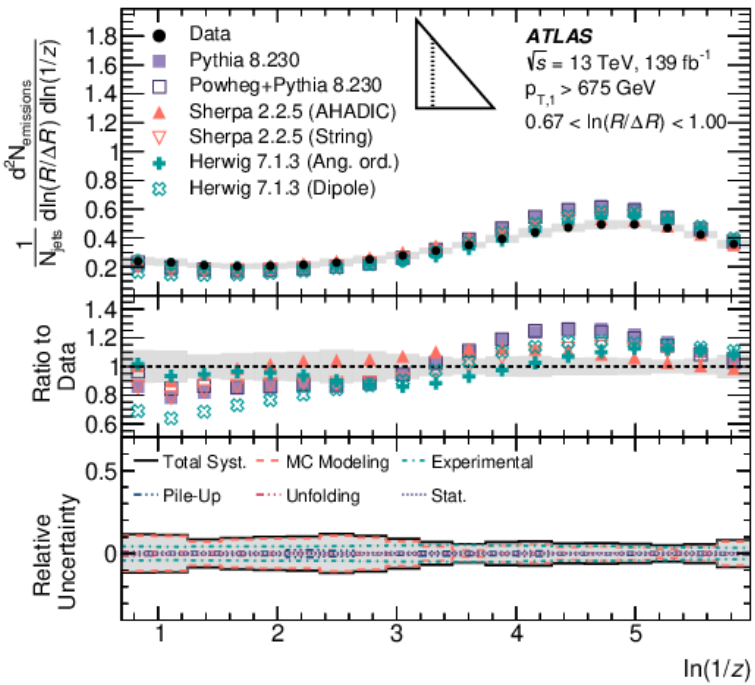


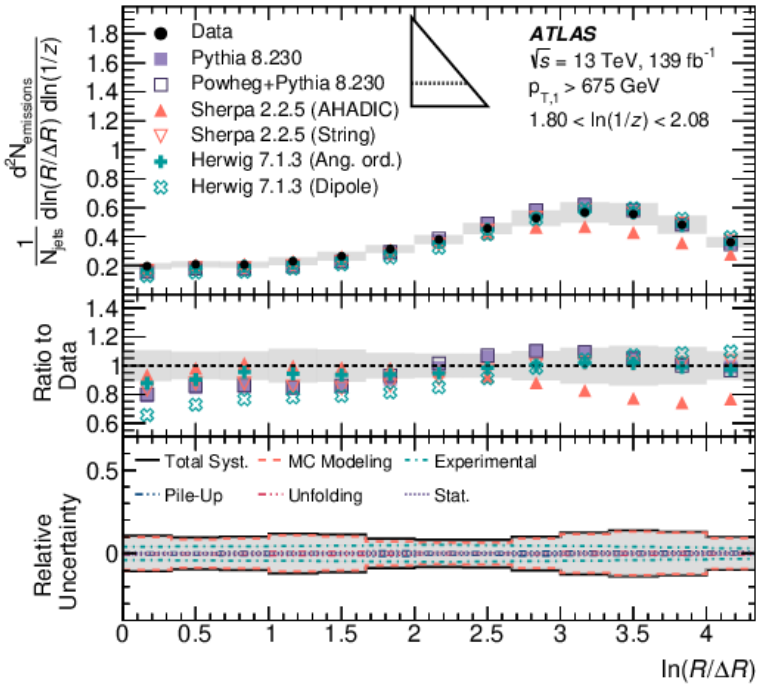


ATLAS Coll., arXiv:2004.03540

# Photon isolation techniques

The isolation requirement mostly suppresses the contribution of photons inside jets.

- A **fixed-cone isolation** can be applied at experimental and theoretical level.

  The isolation energy $E_{\mathrm{T}}^{\mathrm{iso}} \equiv \sum_i E_{\mathrm{T},i}$ sums over particles inside a cone of radius $R^{\mathrm{iso}}$ around the photon direction excluding the photon itself. Isolated photons satisfy the requirement $E_{\mathrm{T}}^{\mathrm{iso}} < E_{\mathrm{T,max}}^{\mathrm{iso}}(E_{\mathrm{T}}^{\gamma})$ where $E_{\mathrm{T,max}}^{\mathrm{iso}}(E_{\mathrm{T}}^{\gamma}) = \epsilon E_{\mathrm{T}}^{\gamma} + E_{\mathrm{T,threshold}}^{\mathrm{iso}}$.

- A **smooth-cone isolation (Frixione's)** can be only applied at theoretical level. The calculations are simplified and any contribution of the parton-to-photon FFs removed.

$$E_{\mathrm{T,max}}^{\mathrm{iso}}(\nu) = \epsilon E_{\mathrm{T}}^{\gamma} \left( \frac{1-\cos\nu}{1-\cos\mathcal{R}} \right)^{n} \quad \text{for all} \quad \nu < \mathcal{R}$$

- A **hybrid-cone isolation** combines a Frixione's isolation of size $\mathcal{R}$ with a fixed-cone of size $R^{\mathrm{iso}}$ for $\mathcal{R}^2 \ll R^{\mathrm{iso},2}$ at theoretical level, reducing their differences.

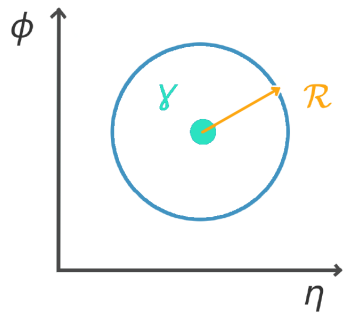


Isolation cone

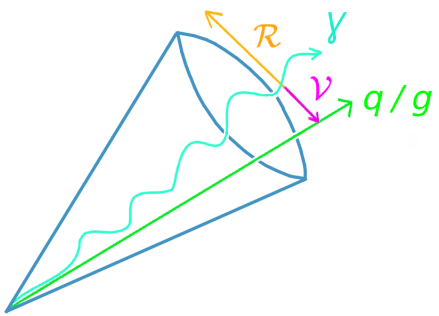

# Inclusive isolated-photon production

Measurement in $pp \to \gamma + X$ processes of the distribution for $E_{\mathrm{T}}^{\gamma}$ in different regions of $|\eta^{\gamma}|$.

- Identification and calibration of photon candidates.
- Isolation requirement of $E_{\mathrm{T}}^{\mathrm{iso}} < 0.0042 \cdot E_{\mathrm{T}}^{\gamma} + 4.8$ GeV.
- Isolated photons with $R^{\mathrm{iso}} = 0.4$ for $E_{\mathrm{T}}^{\gamma} > 125$ GeV and $|\eta^{\gamma}| < 2.37$.
- Data-driven background subtraction.
- Bin-by-bin unfolding technique.

PYTHIA 8.186: ME@LO with NNPDF2.3 LO, $p_{\mathrm{T}}$-ordered PS, Lund string hadr. and A14 tune.
$\Rightarrow$ LO photon-plus-jet hard processes and photon bremsstrahlung in LO QCD dijet events.

The range limited by systematic uncertainties has been extended to $E_{\mathrm{T}}^{\gamma} \sim 1$ TeV.

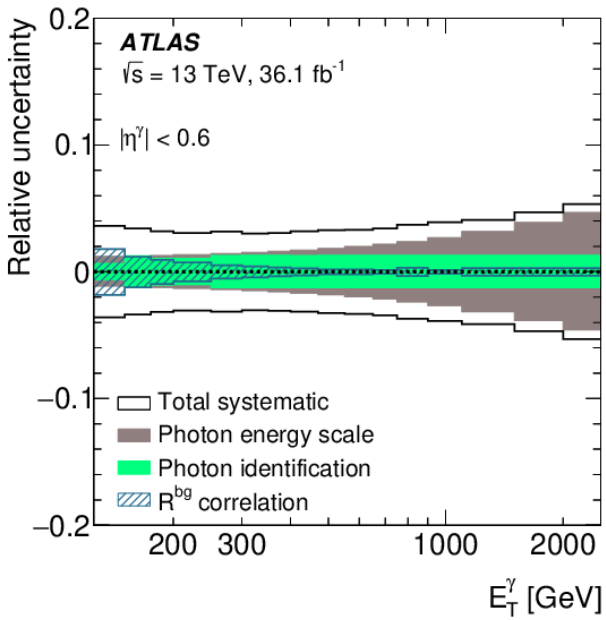


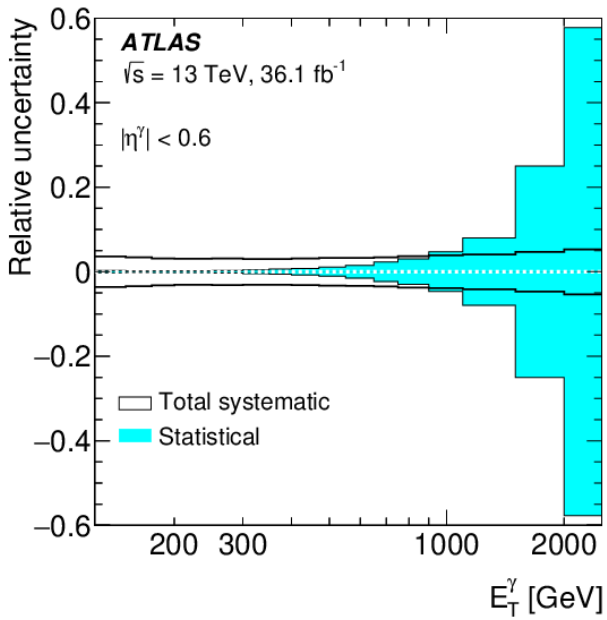


ATLAS Coll., arXiv:1908.02746

# Inclusive isolated-photon production

Theoretical predictions are corrected from non-pQCD effects and not from EW effects.

- **JetPhox:** fixed-order NLO pQCD for $\mu = E_T^\gamma$ and $\mu = E_T^\gamma/2$ with fixed-cone isolation.
  NLO PDFs: MMHT2014, CT14, NNPDF3.0, HERAPDF2.0, ABMP16 $\oplus$ FFs: BFG set II
- **NNLOJet:** fixed-order NNLO pQCD for $\mu = E_T^\gamma$ with hybrid-cone isolation.
  NNLO PDFs: NNPDF3.1. Ref. [arXiv:1904.01044].

The data are adequately described within the uncertainties. This measurement represents a precise test of QCD at NNLO and has the potential to further constrain the PDFs.

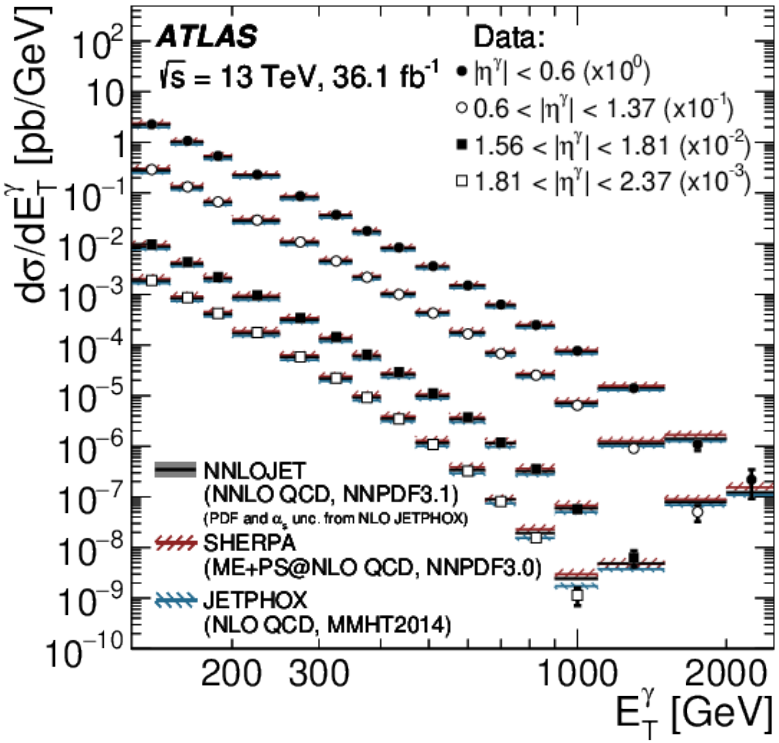


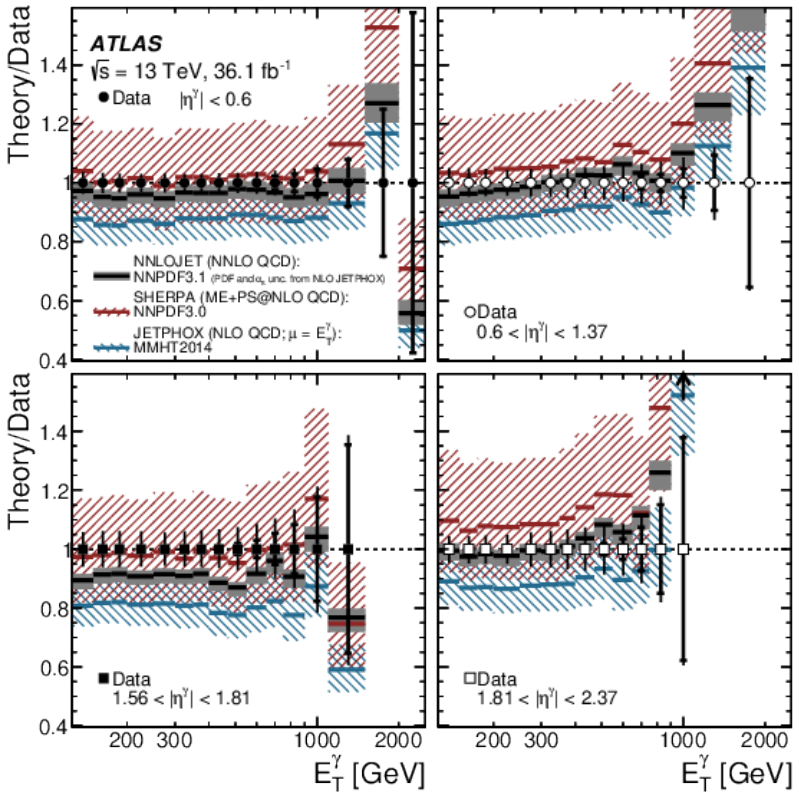


ATLAS Coll., arXiv:1908.02746

# Isolated-photon plus two-jet production

Measurement in $pp \to \gamma + \text{jet} + \text{jet} + X$ processes of the kinematic-variable distributions for $E_{\text{T}}^{\gamma}$, $p_{\text{T}}^{\text{jet}}$, $|y^{\text{jet}}|$, $|\Delta y^{\gamma\text{-jet}}|$, $\Delta\phi^{\gamma\text{-jet}}$, $|\Delta y^{\text{jet-jet}}|$, $\Delta\phi^{\text{jet-jet}}$, $m^{\text{jet-jet}}$ and $m^{\gamma\text{-jet-jet}}$.

The angular correlations and mass distributions probe the dynamics of the hard interaction.

---

- Anti-$k_t$ jets with $R^{\text{jet}} = 0.4$ for $p_{\text{T}}^{\text{jet}} > 100$ GeV and $|y^{\text{jet}}| < 2.5$.
- Isolated photons with $R^{\text{iso}} = 0.4$ for $E_{\text{T}}^{\gamma} > 150$ GeV, $|\eta^{\gamma}| < 2.37$ and $\Delta R^{\gamma\text{-jet}} > 0.8$.
- Multi-jet background subtraction.
- Iterative Bayesian unfolding technique.

SHERPA 2.1.1: ME+PS@LO with CT10 NLO, Frixione's criterion, cluster hadr. and CT10 tune.
$\Rightarrow (2 \to n)$ processes at LO with $n$ from 2 to 5 where bremsstrahlung is accounted for $n \geq 3$.

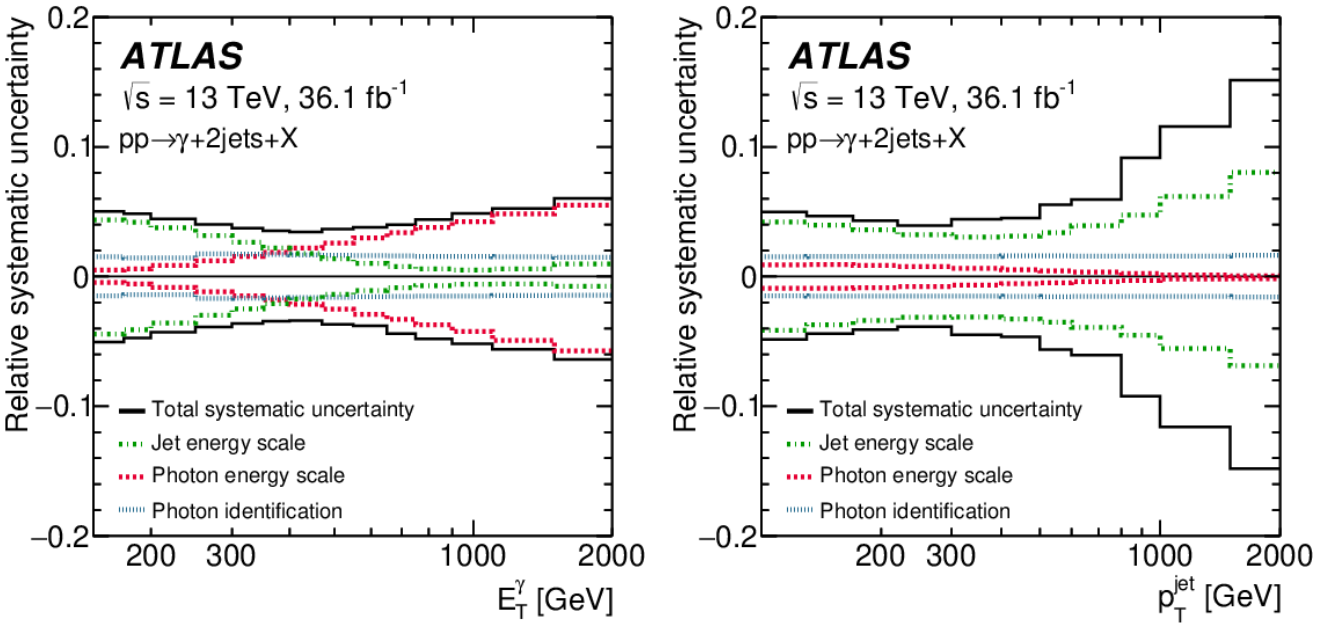


ATLAS Coll., arXiv:1912.09866

# Isolated-photon plus two-jet production

The photon plus two-jet analysis provides a deeper understanding of the underlying production mechanisms for prompt photons.

The inclusive phase space is divided in two regions sensitive to these mechanisms:

- **Direct-enriched** phase space for $E_{\mathrm{T}}^{\gamma} > p_{\mathrm{T}}^{\mathrm{jet}_1}$.
- **Fragmentation-enriched** phase space for $E_{\mathrm{T}}^{\gamma} < p_{\mathrm{T}}^{\mathrm{jet}_2}$.

---

Data are described adequately at NLO in shape and normalization within the uncertainties.

**Inclusive** **Direct** **Fragmentation**

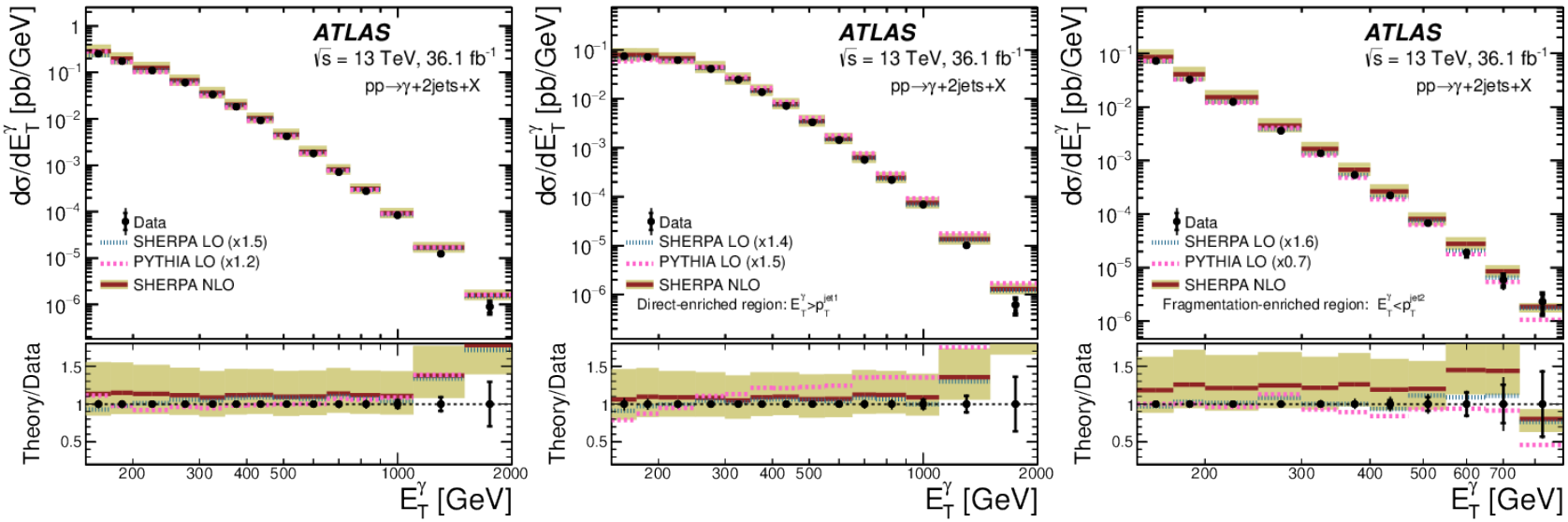


ATLAS Coll., arXiv:1912.09866

# Conclusions

A set of ATLAS measurements from *pp* collisions at $\sqrt{s} = 13$ TeV are presented:

- **Soft-drop jet substructure observables:** all of MC predictions and analytical calculations provide a good description of the data in the resummation region.

  Analytical predictions for jet substructure have only recently been possible following the development of the soft-drop grooming algorithm.

- **Lund jet plane:** the different physical processes are separated in the plane so this measurement provides useful feedback for improving simulations at the LHC.

- **Inclusive isolated-photon production:** the predictions provide a good description of data within the experimental and theoretical uncertainties.

  The NNLO QCD prediction gives an excellent description of the data which have the potential to further constrain the PDFs within a global NNLO QCD fit.

- **Isolated-photon plus two-jet production:** the distributions exhibit the features expected but theoretical uncertainties are much larger than the experimental ones, preventing a more precise test of the theory.

# Backup Slides

# Soft-drop jet observables

**Soft-drop grooming technique:** wide-angle and soft constituents inside jets are removed.
$\Rightarrow$ Less sensitivity to pileup, final-state radiation and underlying event.

$$e_2^{(2)}\Big|_{pp} = \frac{1}{p_{\mathrm{T,jet}}^2} \sum_{i<j\in\mathrm{jet}} p_{\mathrm{T},i} p_{\mathrm{T},j} (\Delta R_{i,j})^2 = \frac{m_{\mathrm{jet}}^2}{p_{\mathrm{T,jet}}^2} \quad \text{where} \quad m_{\mathrm{jet}}^2 = \left( \sum_{i\in\mathrm{jet}} p_i \right)^2$$

The jet mass can be computed using all particles (calorimeter-based) or only charged particles (track-based) as input objects, but the former leads to larger experimental uncertainties.

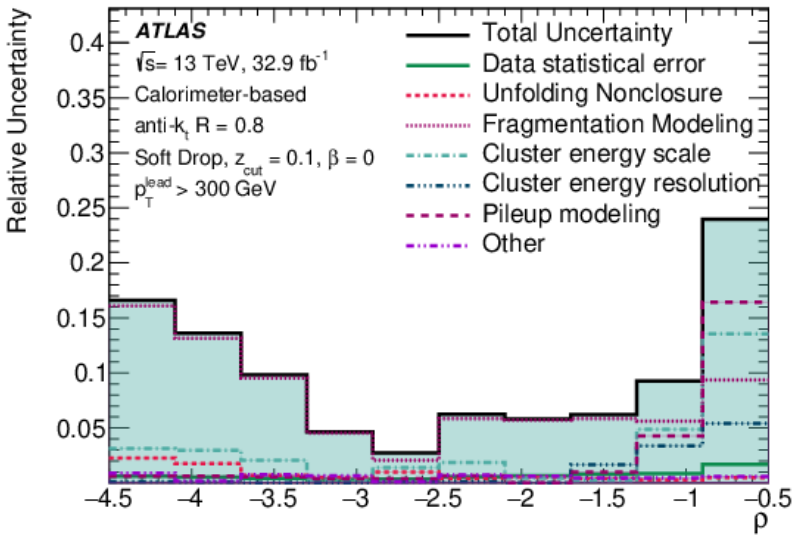


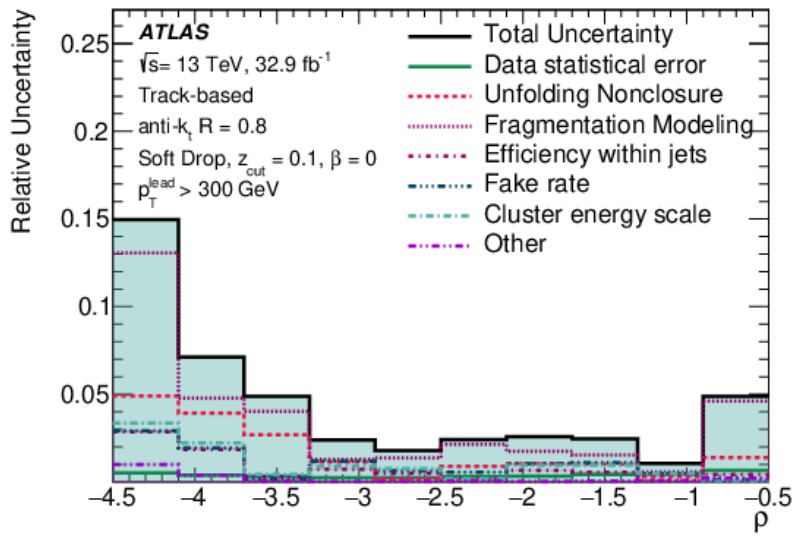


ATLAS Coll., arXiv:1912.09837

# Soft-drop jet observables

Soft-drop measurements are performed in the forward and central regions.

In dijet systems, the jet with smaller $|\eta|$ is the “central” jet and the other one is the “forward” jet. It’s observed that at fixed $p_T$ distributions depend on the initiating parton flavour but not on $|\eta|$.

$\Rightarrow$ They are used to extract quark and gluon jet shapes using the predicted quark and gluon fractions in jet $p_T$ for each $|\eta|$ region.

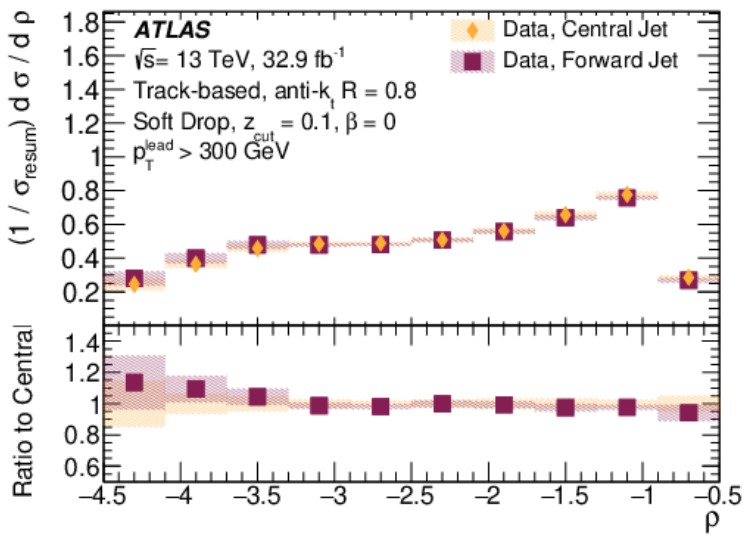


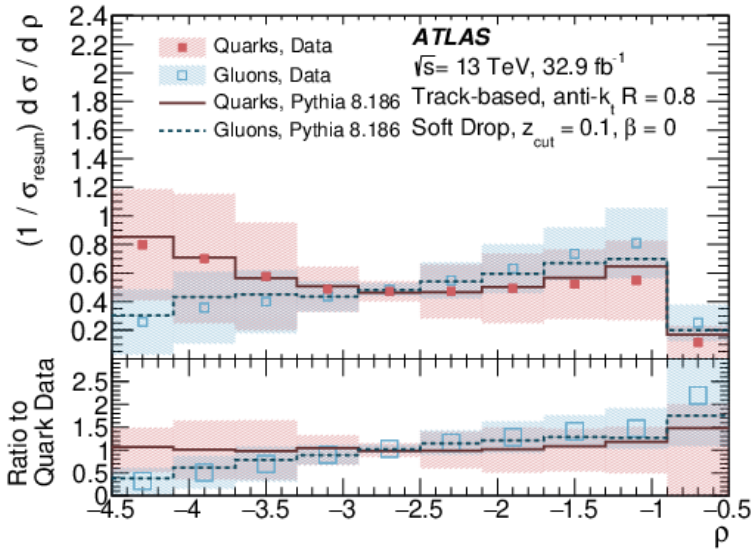


ATLAS Coll., arXiv:1912.09837

---

Jet substructure measurements from the LHC so-far.

Jet substructure physics briefing from April 2020.

# Isolated-photon plus two-jet production

The photon plus two-jet analysis provides a deeper understanding of the underlying production mechanisms for prompt photons.

The inclusive phase space is divided in two regions sensitive to these mechanisms:

- **Direct-enriched** phase space for $E_{\mathrm{T}}^{\gamma} > p_{\mathrm{T}}^{\mathrm{jet}_1}$.
- **Fragmentation-enriched** phase space for $E_{\mathrm{T}}^{\gamma} < p_{\mathrm{T}}^{\mathrm{jet}_2}$.

---

Data are described adequately at NLO in shape and normalization within the uncertainties.

**Inclusive** **Direct** **Fragmentation**

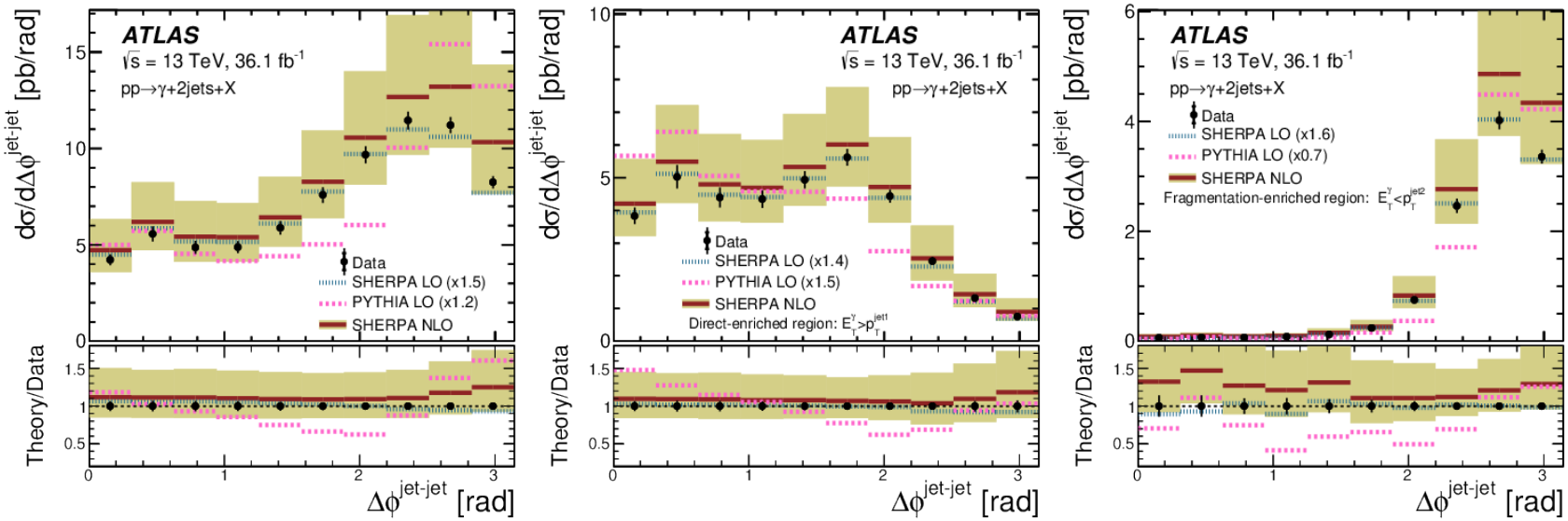


ATLAS Coll., arXiv:1912.09866